Kinetics of H_2S Absorption into Aqueous Ferric Solutions of EDTA and HEDTA

Harm J. Wubs and Antonie A. C. M. Beenackers
Dept. of Chemical Engineering, University of Groningen, Nijenborgh 4, 9747 AG Groningen, Netherlands

Kinetics of the reaction of hydrogen sulfide with ferric chelates of ethylenediaminetetraacetic acid (EDTA) at 22°C and with ferric chelates of hydroxyethylethylenediaminetriacetic acid (HEDTA) from 21°C to 60°C were studied in a stirred cell reactor under industrial conditions. Concentration of the ferric chelates ranged from 40 to 150 mol/m³ and the pH was varied from 4 to 10. Only the hydroxy forms of the ferric chelates appear to react with hydrogen sulfide. Under the conditions applied, the reaction appeared to be first-order in hydrogen sulfide and first-order in hydroxy ferric chelate. At 22°C the rate constant for the EDTA complex is 14-21 m³/mol·s. Uncertainty in this constant is due to the characteristics of the EDTA complex at pH values above 7. For the HEDTA complex, the activation energy of the reaction of hydrogen sulfide with the monohydroxy ferric chelate is (26.4±0.6) kJ/mol with $k_{II}^{m} = 1.8$ *m³/mol·s at 25°C. The rate constant for the reaction with the dihydroxy ferric chelate is (300±150) m³/mol·s in the temperature range investigated.*

Introduction

Many commercial processes are available for the removal of hydrogen sulfide from gaseous streams. Most of these processes use gas-liquid contactors in which the hydrogen sulfide is contacted with a reagent to give either another dissolved sulfide-containing component (for example, alkanol-amine or hydroxide based processes) or elemental sulfur as a precipitate. Important representatives of the latter type are the so-called iron chelate based processes. The absorption of hydrogen sulfide in reactive iron chelate solutions is usually represented by:

$$\begin{aligned} &H_2S(g) \leftrightarrow H_2S(aq) \\ &H_2S(aq) + 2Fe^{3+}\text{Chelant}^{n-} \rightarrow S\downarrow + 2H^+ + 2Fe^{2+}\text{Chelant}^{n-} \end{aligned} \tag{1}$$

In this equation, the number n denotes the charge of the chelant anion. For HEDTA, n has a value of 3 and for EDTA a value of 4. Since the active ferric chelate is converted to inactive ferrous chelate, the latter component has to be regenerated into its ferric form by oxidation of the solution with oxygen:

$$\begin{aligned} &O_2(g) \leftrightarrow O_2(aq) \\ &O_2(aq) + 4Fe^{2+}\text{Chelant}^{n-} + 2H_2O \rightarrow 4Fe^{3+}\text{Chelant}^{n-} + 4OH^- \end{aligned} \tag{2}$$

This way, the iron chelate can be regarded as a pseudocatalyst in the reaction of hydrogen sulfide with oxygen (Buenger et al., 1987). The sulfur produced is easily recoverable from the slurry. Another advantage of iron chelate based processes is that they essentially operate at ambient conditions. An overview of some key features of iron chelate based processes as can be obtained from patent and literature data is presented in Table 1.

Table 1. Typical Operation Conditions of Iron Chelate Based Processes

Temperature	20-60°C
pH	6-9
Pressure	< 100 bar
Important chelants	EDTA, HEDTA, NTA
Iron chelate concentration	10-1,000 mol/m³
Chelant/iron ratio	1.1-1.6

Correspondence concerning this article should be addressed to A. A. C. M. Beenackers.

Although patents on these processes have existed for more than 15 years already, actual kinetic data on the reaction of hydrogen sulfide with iron chelates were not available until the recent results of DeBerry et al. (1991). These authors used a stopped-flow method combined with spectrophotometric analysis to measure the kinetics of the reaction of hydrogen sulfide with iron chelates of EDTA and, though in less detail, with the chelates of HEDTA, diethylenetriaminepentaacetic acid (DTPA) and ethylene bis(oxyethylenenitrilo)tetraacetate (EGTA). The total concentration of sulfide, that is, bisulfide and hydrogen sulfide together, ranged from 0.25 mol/m^3 up to 10 mol/m^3 and the concentration of the ferric chelate from 0.25 mol/m^3 up to 25 mol/m^3, which covers only the very low end of the working range of commercial iron chelate processes. The pH was maintained between 6.0 and 8.0 and the results reported are limited to 10°C only. Both for EDTA and HEDTA, DeBerry et al. (1991) observed the conversion of hydrogen sulfide to sulfur to proceed through the formation of an iron chelate bisulfide complex (Fe^{3+}L-SH). For EDTA, the reaction rate initially was first-order in ferric EDTA and first-order in hydrogen sulfide. No reaction orders were reported for the other iron chelates studied, although from the reaction rate constants given, first-order dependency in ferric chelate may be assumed. Also, the temperature dependency of the reaction rate constants is unknown yet. The reaction rate seems to be independent of the ionic strength, and the pH dependency found possibly can be ascribed to the reactive species being hydroxy ferric chelate (DeBerry et al., 1991).

Other systems in which hydrogen sulfide is converted to sulfur by ferric iron are described by Novikov et al. (1984) and Asai et al. (1990). The former authors absorbed hydrogen sulfide into an aqueous solution of ferric chloride and found the reaction to be first-order in both ferric iron and hydrogen sulfide. Also, a dependency on the concentration of chloride ions was observed. For an aqueous solution containing ferric sulfate, Asai et al. (1990) also concluded that the reaction was first-order both in ferric iron and hydrogen sulfide. The pH dependency found by these authors was ascribed to the reactive species, reportedly by the monohydroxy form of ferric iron. In accordance with DeBerry et al. (1990), the observed reaction rate was independent of the ionic strength of the solution.

It is the aim of this work to establish the reaction kinetics of hydrogen sulfide with ferric chelates of EDTA and HEDTA. The reaction order in both ferric chelate and hydrogen sulfide will be determined together with the active form of ferric chelate and the possible influence of a reaction between hydrogen sulfide and hydroxide, if any.

Experimental

The experimental setup is the same as described previously (Wubs and Beenackers, 1993). Stock solutions were made in various ways, depending on the pH range used during the experiment. For experiments at low pH below 5.5, ferric chloride was dissolved and EDTA and HEDTA added up to a ratio of chelant/Fe = 1.1. EDTA and HEDTA stock solutions had a concentration of about 0.2 and 1.0 kmol/m^3, respectively. Prior to use, NaCl was dissolved in half a liter of reverse osmosis purified water to give a total chloride concentration of 3 kmol/m^3 after addition of the iron chelate solution and diluting to 1,000 mL. An amount of stock solution of ferric chelate was added and the solution was further diluted to about 950 mL. Then, an amount of sodium hydroxide solution (with a concentration of 4 kmol/m^3) was added to adjust the pH. After adjustment, the solution was diluted to 1,000 mL. Since adjusting to higher pH values led to the precipitation of ferric hydroxide, stock solutions were made in the latter case by adding ferrous chloride to the solutions of chelant whereafter the pH was adjusted to pH = 10. Subsequently, the solution was regenerated with air to give the respective ferric complex. If the latter solution had a too high pH value, hydrochloric acid was used to adjust the pH prior to use.

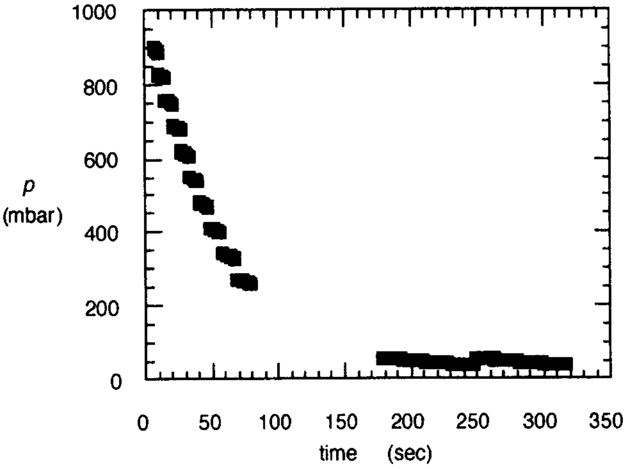

Figure 1. Typical experimental absorption curves.

After filling the reactor with the desired iron chelate solution containing 3 kmol/m^3 NaCl, it was evacuated. Once the solution was equilibrated under its own vapor pressure, hydrogen sulfide was added until a maximum pressure of 950 mbar was reached. This typically took less than 5 s. After 10 mbar of hydrogen sulfide was absorbed, the reactor pressure was rapidly reduced by 70 mbar, and another 10 mbar of hydrogen sulfide was allowed to absorb. Thus, about 9 absorption cycles were obtained at a relatively high mean pressure, each cycle having an average pressure of about 80 mbar lower than the previous one. At a total pressure of about 250 mbar, the reactor pressure was reduced to somewhat in excess of 35 mbar above the vapor pressure of water. Then 20 mbar of hydrogen sulfide was absorbed, followed by addition of a small amount of hydrogen sulfide to the reactor to reach again a pressure somewhat in excess of 35 mbar to repeat the last cycle. This way, information on the absorption rate of hydrogen sulfide into the aqueous solution could be obtained both at relatively high and low hydrogen sulfide pressures without significant conversion of the ferric chelate or change in pH. A typical pressure vs. time curve thus obtained is shown in Figure 1. The experiment was followed by determination of the mass-transfer coefficient using nitrous oxide and by analysis of the amount of ferric iron present in solution, as described previously (Wubs and Beenackers, 1993).

As during experiments, sulfur is formed according to Eq. 1 the gas-liquid interface may get covered by sulfur thus blocking the transfer of hydrogen sulfide. To prevent this, the stirrer speed was set to 1,200 rpm. This resulted in a turbulent but sulfur free interface. Higher stirrer speeds led to vortex formation whereas it was observed that at lower stirrer speeds

Table 2. Mass-Transfer Properties for Hydrogen Sulfide Absorption into Iron Chelate Solutions*

Chelant	T °C	E_{CO_2} at rpm 300	E_{CO_2} at rpm 1,200	$E_{CO_2\infty}$ min	$E_{CO_2\infty}$ max	$10^3\ k_La$ s^{-1}	a/a_0 -	$10^4\ k_L$ m/s
EDTA	22.1	75	7	310	770	1.69±0.03	1.64±0.02	1.23
HEDTA	21.5	75	7	310	770	1.75±0.03	1.64±0.02	1.27
	42.0	100	12	450	1,100	2.34±0.02	1.58±0.02	1.77
	60.3	120	16	560	1,400	2.67±0.07	1.51±0.02	2.11

* $a_o = 8.37\ m^2/m^3$ at 300 rpm. $E_{CO_2\infty}$ is calculated from Eq. 10b.

indeed sulfur deposited at the gas-liquid interface. By absorbing carbon dioxide into 3 kmol/m^3 NaCl solutions containing sodium hydroxide, the net increase of the gas-liquid contact area with respect to a flat interface could be measured.

Mass-Transfer Properties

To calculate both the kinetic data and the diffusivities of the ferric chelates, the mass-transfer coefficients, the gas-liquid interfacial area and the gas solubilities should be known. Determination of the solubility of hydrogen sulfide in ferrous chelate solutions is not accurate, because in the absence of ferric chelate, ferrous chelate can be converted into ferrous sulfide. Therefore, the solubility was obtained indirectly from experiments in the instantaneous reaction regime as in this regime besides diffusivities also the solubility of hydrogen sulfide can be obtained. The following section covers this subject in more detail. Also mass-transfer coefficients were obtained indirectly from following the physical absorption of N_2O with time. The value of k_La follows from:

$$\left(\frac{k}{k+1}\right)\ln\left(\frac{p_A^0}{(k+1)p_A - kp_A^0}\right) = k_Lat \text{ with } k = \left(\frac{V_GHe}{V_LRT}\right) \quad (3)$$

by linear regression techniques. The value of k_La thus found for N_2O is converted to k_La for hydrogen sulfide via:

$$(k_La)_{H_2S} = (k_La)_{N_2O}\cdot\sqrt{\frac{D_{H_2S}^{water}}{D_{N_2O}^{water}}} \quad (4)$$

The diffusivity of nitrous oxide in water is given by Versteeg and van Swaaij (1988). The diffusivity of hydrogen sulfide in water was calculated from the equation of Haimour and Sandall (1984), which is more accurate than that of Wilke and Chang (1955).

The interfacial contact area at high stirrer speeds where the gas-liquid interface is no longer flat, was obtained from the absorption rate of carbon dioxide into a 3 kmol/m^3 NaCl solution containing 0.1 kmol/m^3 NaOH, the pressure of carbon dioxide varying between 35 mbar and 15 mbar. Due to the presence of sodium hydroxide, the absorption of carbon dioxide is enhanced relative to physical absorption. Since the reaction of carbon dioxide with the hydroxide species is first-order in carbon dioxide, as was checked, the pressure changes with time according to:

$$\ln\left(\frac{p_A^0}{p_A}\right) = \frac{V_LRT}{V_GHe}\cdot k_La\cdot E_A\cdot t \quad (5)$$

If $2 \ll E_A \ll E_{A\infty}$, then $E_A = Ha$ (Westerterp et al., 1984) and Eq. 5 reduces to:

$$\ln\left(\frac{p_A^0}{p_A}\right) = \frac{V_LRT}{V_GHe}\cdot a\sqrt{k_{AB}D_Af(C_A^i, C_B)}\cdot t \quad (6)$$

Here, $f(C_A^i, C_B)$ depends on the reaction kinetics only. For first order in both CO_2 (A) and OH^- (B), $f(C_A^i, C_B)$ reduces to C_B. In that case the only variable dependent on the stirrer speed is the interfacial area a. Checks revealed that indeed this condition, that is, $2 \ll E_A \ll E_{A\infty}$, was fulfilled, see Table 2. By carrying out experiments with an absorption curve at a high stirrer speed immediately followed by a similar curve at such a low stirrer speed that the interface is flat, the increase of the interfacial area can be calculated relative to the known flat area without exact knowledge of the reaction kinetics as long as the concentration change of hydroxide remains negligible. The results thus obtained for k_La, a and k_L are presented in Table 2.

Results

As follows from Figure 1, experimental results have been obtained both at relatively high and low hydrogen sulfide pressures. In the high pressure regime, the pressure drop during the experiment is negligibly small with respect to the average pressure so that the average pressure can be considered as constant. In the low pressure regime, however, the pressure change is of the same order of magnitude as the average pressure and the latter cannot be considered as constant. Therefore, these regimes are treated differently.

Using the ideal gas law, the absorption rate of hydrogen sulfide into the liquid can be related to the pressure change via:

$$J_AaV_L = \frac{V_G}{RT}\cdot\left(-\frac{dp_A}{dt}\right) \quad (7)$$

The absorption rate J_A depends on the mass-transfer rate of hydrogen sulfide into the liquid and on the reaction rate with ferric chelate according to:

$$J_A = k_LE_AC_A^i \quad \text{with} \quad C_A^i = p_A/He \quad (8)$$

From this it follows:

$$\left(-\frac{dp_A}{dt}\right) = \frac{V_LRT}{V_GHe}\cdot k_La\cdot E_A\cdot p_A \quad (9)$$

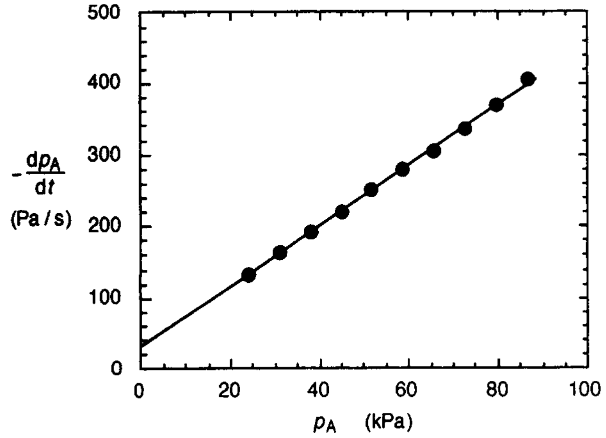

Figure 2. Absorption rate of hydrogen sulfide as function of the hydrogen sulfide pressure.

Experimental conditions: $T = 295.3$ K, $C_B = 93.2$ mol/m³. Correlation coefficient is 0.999.

Depending on the mass transfer with reaction regime the enhancement factor E_A may take a different form. If the enhancement factor does not depend on p_A, integration will lead to Eq. 5. In the following subsections the high pressure regime and the low pressure regime will be discussed separately.

High pressure regime

Since in the high pressure regime the average pressure during an experiment remains approximately constant, a linear decrease of the pressure with time is observed in each experiment. According to Eq. 9 a plot can be made of the slope of each curve, that is, $(-dp_A/dt)$ vs. p_A. A typical result is shown in Figure 2, from which it follows that a clear linear relationship exists between the absorption rate of hydrogen sulfide and the hydrogen sulfide partial pressure. As the intercept of the line through the data points does significantly deviate from zero, it follows that the enhancement factor E_A equals the enhancement factor for instantaneous reaction $E_{A\infty}$. We found (Wubs and Beenackers, 1993) the film model appropriate to describe the instantaneous reaction between oxygen and ferrous chelate. Therefore, the same expression may hold for instantaneous reaction between hydrogen sulfide and ferric chelate:

$$E_A = E_{A\infty} = 1 + \frac{D_B C_B^a}{\nu_B D_A C_A^i} = 1 + He\frac{D_B C_B^a}{\nu_B D_A p_A} \qquad (10a)$$

For penetration theory, Chang and Rochelle (1982) developed a similar expression for the instantaneous enhancement factor:

Table 3. Solubility of Hydrogen Sulfide in Ferric Chelate Solutions*

Chelant	Temp. °C	Slope × 10³ s⁻¹	*He* kPa·m³/mol
EDTA	22.1	4.25 ± 0.15	1.25
HEDTA	21.5	4.18 ± 0.15	1.31
	42.0	4.62 ± 0.15	1.69
	60.3	4.92 ± 0.34	1.92

* $V_L = 9.96 \times 10^{-4}$ m³; $V_G = 7.81 \times 10^{-4}$ m³.

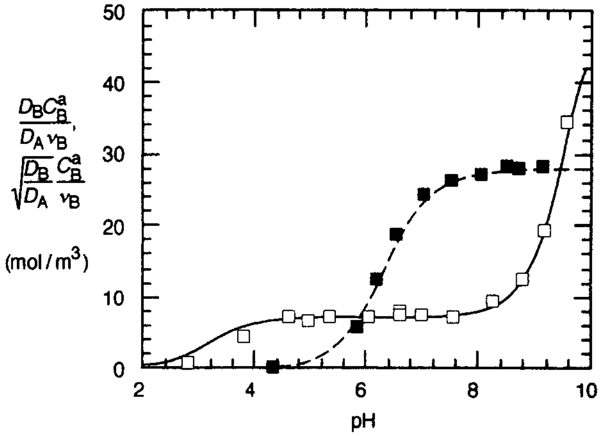

Figure 3. $(D_BC_B^a)/(\nu_BD_A)$ and $(\sqrt{D_B}C_B^a)/(\nu_B\sqrt{D_A})$ as function of pH for the ferric chelate of EDTA (■) at 22.1°C and the ferric chelate of HEDTA (□) at 21.5°C.

The total concentration of ferric chelate is 95 mol/m³. The lines are calculated from Eqs. 15 to 17 with the data tabulated in Table 4; ——: FeHEDTA; ----: FeEDTA.

$$E_A = E_{A\infty} = 1 + \sqrt{\frac{D_B}{D_A}}\frac{C_B^a}{\nu_B C_A^i} = 1 + He\sqrt{\frac{D_B}{D_A}}\frac{C_B^a}{\nu_B p_A} \qquad (10b)$$

Substituting the Eqs. 10 into Eq. 9 leads to:

$$\left(-\frac{dp_A}{dt}\right) = \frac{V_L RT}{V_G He}\cdot k_L a\cdot\left(p_A + He\frac{D_B C_B^a}{\nu_B D_A}\right) \qquad (11a)$$

$$\left(-\frac{dp_A}{dt}\right) = \frac{V_L RT}{V_G He}\cdot k_L a\cdot\left(p_A + He\sqrt{\frac{D_B}{D_A}}\frac{C_B^a}{\nu_B}\right) \qquad (11b)$$

for film model and penetration theory, respectively. As the diffusivity of nitrous oxide and hydrogen sulfide are close to each other, Eq. 4 can be used for the calculation of k_La for both Eq. 11a and Eq. 11b without causing significant errors.

In these equations, C_B^a denotes the concentration of the active components of ferric chelate, because some of the forms in which ferric chelate can appear, depending on pH, may not react with hydrogen sulfide. Checks revealed that the slope of $(-dp_A/dt)$ vs. p_A depends neither on pH nor on the total iron concentration C_B. This is in agreement with Eq. 11, and therefore, in the light of Figure 2, it is concluded that indeed the reaction between the hydrogen sulfide and iron chelate is instantaneous in the high hydrogen sulfide pressure regime. As both the mass-transfer coefficient and the gas and liquid volumes are known, the solubility of hydrogen sulfide in the reactive solution can be calculated from the slope. The results are given in Table 3. From the intercept of each line $(D_BC_B^a)/(\nu_BD_A)$ or $(\sqrt{D_B}C_B^a)/(\nu_B\sqrt{D_A})$ are obtained as a function of the pH and the total ferric chelate concentration. Figure 3 presents this number as a function of the pH for the ferric chelates of EDTA and HEDTA. From this figure it appears that the groups $(D_BC_B^a)/(\nu_BD_A)$ and $(\sqrt{D_B}C_B^a)/(\nu_B\sqrt{D_A})$ strongly depend on the pH. Important to notice is that hydrogen sulfide does not seem to react with ferric HEDTA below

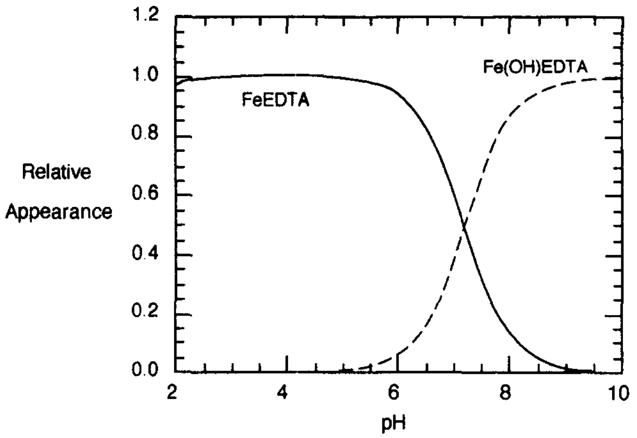

Figure 4. Relative appearance (concentration of a ferric chelate species divided by the total concentration of ferric iron) of ferric EDTA.

a pH of about 2 and with ferric EDTA below a pH of about 5. Therefore, besides reactive forms of ferric chelate also unreactive forms must exist. Figures 4 and 5 show the form of ferric chelate present in solution as a function of pH for the EDTA and HEDTA ferric chelates, respectively. These equilibria were calculated from the data of Gustafson and Martell (1963). Protonated ferric chelate appears in appreciable amounts only below a pH of 2. The comparison of Figures 4 and 5 with Figure 3 suggests that the reactive species is the hydroxy form of the ferric chelate, for both EDTA and HEDTA. Considering the change of the curve for HEDTA in Figure 3 when the monohydroxy form transforms into the dihydroxy form, it is very likely that the dimer of the monohydroxy form is not reactive towards hydrogen sulfide. The inertness of the dimer towards hydrogen sulfide has been suggested earlier by Philip and Brooks (1974). According to the possible configurations of this dimer, as given by Gustafson and Martell (1963), it is plausible indeed that the dimer is not reactive, because the chelants effectively shield the central metal ions from the outside.

The hydroxy equilibria that exist are (Gustafson and Martell, 1963):

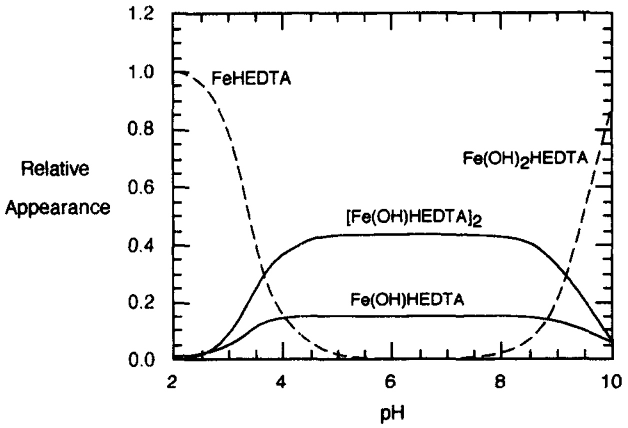

Figure 5. Relative appearance (concentration of a ferric chelate species divided by the total concentration of ferric iron) of ferric HEDTA.

$$\mathrm{Fe}^{3+}L^{n-} + \mathrm{OH}^- \overset{K_A}{\leftrightarrow} \mathrm{Fe}^{3+}(\mathrm{OH}^-)L^{n-} \tag{12}$$

$$\mathrm{Fe}^{3+}(\mathrm{OH}^-)L^{n-} + \mathrm{OH}^- \overset{K_B}{\leftrightarrow} \mathrm{Fe}^{3+}(\mathrm{OH}^-)_2L^{n-} \tag{13}$$

$$2\mathrm{Fe}^{3+}(\mathrm{OH}^-)L^{n-} \overset{K_D}{\leftrightarrow} [\mathrm{Fe}^{3+}(\mathrm{OH}^-)L^{n-}]_2 \tag{14}$$

For the ferric EDTA chelate, only equilibrium 12 is relevant whereas for the ferric HEDTA chelate all equilibria play a role. From these equilibria the concentrations of the mono- and dihydroxy complexes can be calculated:

$$\text{monohydroxy chelate: } C_B^m = 2K_A C_{\mathrm{OH}^-} C_B/\alpha \tag{15}$$

$$\text{dihydroxy chelate: } C_B^d = 2K_A K_B C_{\mathrm{OH}^-}^2 C_B/\alpha \tag{16}$$

with

$$\begin{aligned}\alpha = {} & 1 + K_A C_{\mathrm{OH}^-}(1 + K_B C_{\mathrm{OH}^-}) \\ & + \sqrt{(1 + K_A C_{\mathrm{OH}^-}(1 + K_B C_{\mathrm{OH}^-}))^2 + 8 C_B K_D (K_A C_{\mathrm{OH}^-})^2}\end{aligned} \tag{17}$$

As the curves of Figure 3 are somewhat shifted relative to the curves of Figures 4 and 5, it is not possible to calculate the concentrations of the different species present in solution by using the values given by Gustafson and Martell (1963). Therefore, not only the ratio of diffusivities but also the equilibrium constants are calculated from fitting Eqs. 15 to 17 together with $D_B/\nu_B D_A$, or alternatively $\sqrt{D_B}/\nu_B\sqrt{D_A}$, on the data points of Figure 3. As the ferric EDTA complex has only one hydroxy component in the pH range of interest and because the curve levels off toward a maximum value, the ratio $D_B/\nu_B D_A$, or alternatively $\sqrt{D_B}/\nu_B\sqrt{D_A}$, of $\mathrm{Fe}^{3+}(\mathrm{OH}^-)\mathrm{EDTA}^{4-}$ and K_A are readily obtained from Figure 3.

For ferric HEDTA the situation is more complicated. At intermediate pH values, that is, for the range where the curve is horizontal, the diffusivity ratio $D_B/\nu_B D_A$, or $\sqrt{D_B}/\nu_B\sqrt{D_A}$, cannot be calculated without knowledge of the ratio of the monomer to the dimer of the monohydroxy species. At high pH values, where only the dihydroxy species exists, the curve does not level off, and therefore a separate diffusivity ratio $D_B/\nu_B D_A$, or $\sqrt{D_B}/\nu_B\sqrt{D_A}$, for this species cannot be obtained. Going to still higher pH-values, the curve may probably level off but also ferric hydroxide will precipitate from solution. As a first guess, it can be assumed that the diffusivity of the dihydroxy ferric chelate equals that of the monohydroxy ferric chelate. This assumption is validated by our previous results where it was found that both ferrous EDTA and ferrous HEDTA have the same diffusivity irrespective of a difference in complex ion charge. Since $D_B/\nu_B D_A$ and $\sqrt{D_B}/\nu_B\sqrt{D_A}$ are hardly temperature dependent, the value obtained at 20°C is used to estimate the equilibrium constants at higher temperatures. Table 4 summarizes the results thus obtained. K_B and K_D for FeHEDTA compare very well with the values of Gustafson and Martell (1963). The values found for K_A deviate more, but this may be caused by a difference in experimental conditions. Gustafson and Martell (1963) determined their equilibria constants in a 1 kmol KCl/m^3 solution whereas in this work a 3 kmol NaCl/m^3 solution was applied. The lines drawn in Figure 3 are calculated from the experimental data reported in Table 4. The overall results are presented in Figure

Table 4. Results of Parameter Fits for Diffusivity Ratios and Hydroxy Equilibria*

Chelant	Temp. °C	$D_B/\nu_B D_A$† $\sqrt{D_B}/\nu_B\sqrt{D_A}$‡	Log K_A m^3/kmol	Log K_B m^3/kmol	Log K_D m^3/kmol
EDTA	22.1	0.30	7.78		
HEDTA	21.5	0.49	9.6	5.3	2.3
	42.0	0.49	8.8	5.0	2.0
	60.3	0.49	8.0	4.6	1.9
EDTA**	25.0		6.43		
HEDTA**	25.0		9.90	5.32	2.38

*The latter are compared to the values reported by Gustafson and Martell (1963).

**Gustafson and Martell (1963).

†Film model.

‡Penetration theory.

6. It can be seen that the model developed for the absorption in the instantaneous reaction regime correlates very well with the experiments.

Low pressure regime

In the low pressure regime the absorption curves are different from those obtained in the high pressure regime. Now, the total pressure can no longer be regarded as constant within a single experiment. Therefore, the interpretation of these experiments will differ from those reported in the previous subsection. Again, the pressure drop with time can be correlated to the pressure of hydrogen sulfide by Eq. 9. In case of a first-order reaction in hydrogen sulfide, Eq. 9 can be integrated to give Eq. 5. If a plot of $\ln(p_A^0/p_A)$ vs. time turns out to be linear and its intercept from the y-axis is zero, then E_A is independent of p_A and the reaction is first-order in A. An example for the reaction between hydrogen sulfide and ferric HEDTA is given in Figure 7 which shows that E_A is independent of p_A, thus leading to the conclusion that the reaction is first-order in hydrogen sulfide. Similar plots were obtained for other conditions as well as for the EDTA complex. At higher pH values, above 6, plots like those of Figure 7 tended to show a curvature, indicating that the reaction started to deviate from first order. Above a pH of about 8.5 the reaction of hydrogen sulfide with the ferric chelate of HEDTA turned out to be instantaneous whereas it was slower at intermediate pH values.

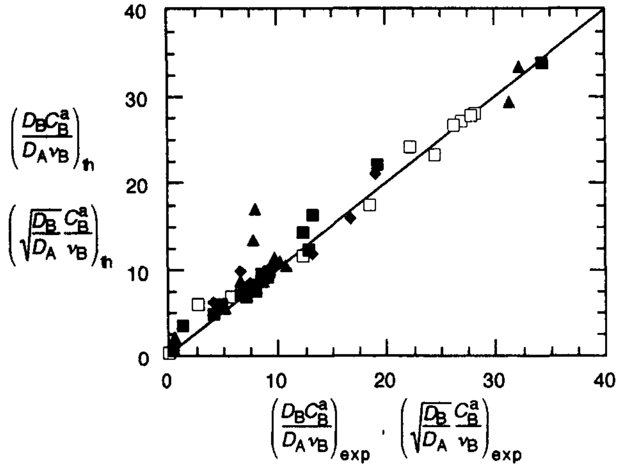

Figure 6. Model value of $(D_B C_B^a)/(\nu_B D_A)$ and $(\sqrt{D_B} C_B^a)/(\nu_B\sqrt{D_A})$ plotted as function of the experimental value of $(D_B C_B^a)/(\nu_B D_A)$ and $(\sqrt{D_B} C_B^a)/(\nu_B\sqrt{D_A})$, respectively.

The theoretical values are calculated from Eqs. 15-17 with the data of Table 4. □: EDTA, $T=22.1$°C, pH = 4-9, $C_B=40$-140 mol/m^3, R.M.S. error = 0.57; ■: HEDTA, $T=21.5$°C, pH = 3-10, $C_B=50$-150 mol/m^3, R.M.S. error = 0.41; ◆: HEDTA, $T=42.0$°C, pH = 5-9, $C_B=50$-150 mol/m^3, R.M.S. error = 0.28; ▲: HEDTA, $T=60.3$°C, pH = 4-9, $C_B=50$-150 mol/m^3, R.M.S. error = 0.72.

To cover the whole range from slow reaction to instantaneous reaction, Eq. 9 was integrated numerically for each experimental curve. The slow to fast reaction regime was dealt with by using the Danckwerts-model (Westerterp et al., 1985) for the calculation of the enhancement factor E_A and the intermediate regime between fast and instantaneous reaction by using the DeCoursey-model (DeCoursey, 1974). The instantaneous reaction regime was covered by Eq. 10. The latter equation was also applied in the DeCoursey-model. From both the Danckwerts-model and the DeCoursey-model the reaction rate constants are obtained in form of a Hatta-number:

$$Ha=\sqrt{\frac{D_A k_{1m} C_B^m}{k_L^2}} \tag{18}$$

in which m is the reaction order in ferric chelate. DeBerry et al. (1991) showed that with the ferric EDTA complex, the

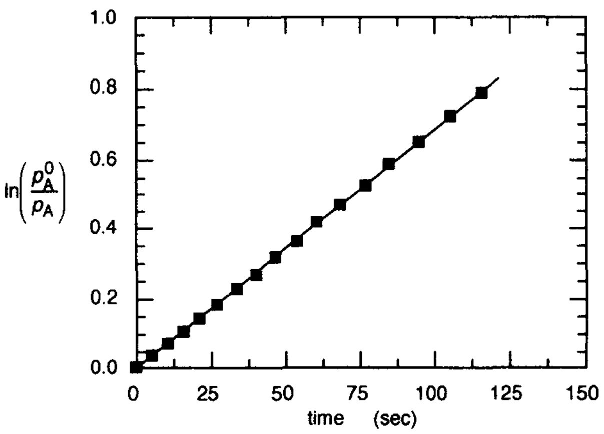

Figure 7. Ln(p_A^0/p_A) as function of time: a linear dependency.

Conditions: $C_{Fe^{3+}\text{-}HEDTA}=70$ mol/m^3; pH = 5.03; $T=21.5$°C. Correlation coefficient = 0.9999.

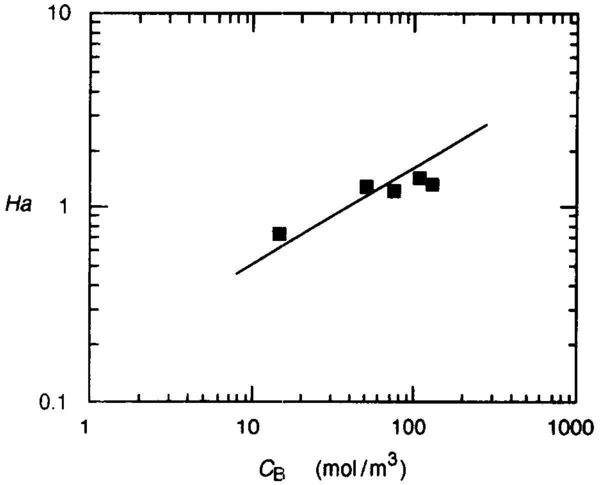

Figure 8. Hatta number as function of the concentration of the ferric HEDTA complex.

$T = 21.5°C$, R.M.S. error = 0.21.

reaction is first-order in iron chelate, m thus being 1. Figure 8 shows a plot of the experimentally observed Hatta-number for the ferric HEDTA complex as a function of the total ferric iron chelate present in solution. The slope of approximately one half indicates that also ferric HEDTA reacts according to first-order kinetics in ferric chelate.

Figure 9 shows the dependency of the Hatta-number on the pH. The characteristics are similar to those found at higher hydrogen sulfide pressures, as reported above. Since all the experimental results reported in Figure 9 were obtained at the same concentration of ferric iron complex and at about the same temperature, it can be concluded that monohydroxy ferric HEDTA is less reactive than the corresponding EDTA complex (see also Figures 4 and 5). The dihydroxy form, however, appears to be much more reactive, still. Due to the limited number of experimental data above a pH of 8, accurate determination of the reaction rate constant for the dihydroxy component is not possible yet. Moreover, these experiments were hampered by a low concentration of that species so that minor experimental errors resulted in major deviations in the reaction rate constant. The reaction rate constants as obtained from the Hatta-number are presented in Table 5.

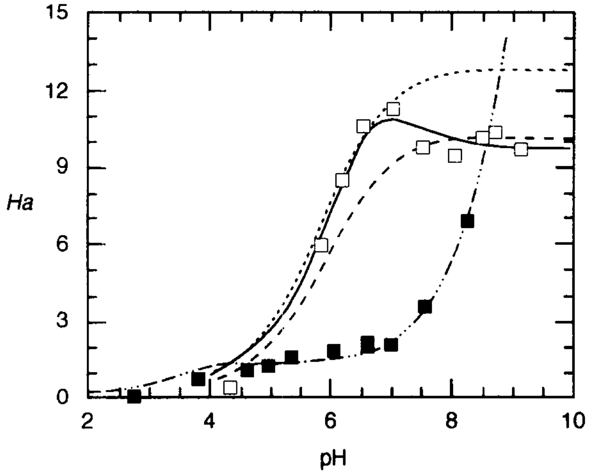

Figure 9. Dependency of the Hatta number on the pH of the solution at 22.1°C for the ferric chelate of EDTA (□) and at 21.5°C for the ferric chelate of HEDTA (■).

The total ferric iron concentration is 78 mol/m^3. ------: EDTA, calculated with $k_{11}^{m} = 21$ m^3/mol·s and K_A from Table 4; ----: EDTA, calculated with $k_{11}^{m} = 14$ m^3/mol·s and K_A from Table 4; ——: EDTA, best line; -·-·-·: HEDTA, calculated with data from Tables 4 and 5.

Table 5. Observed Reaction Rate Constants Compared to the Values Reported at pH = 6.5 by DeBerry et al. (1991)*

Chelant	Temp. °C	k_{11}^{m} m^3/mol·s	k_{11}^{d} m^3/mol·s	$10^9 D_A$ m^2/s
EDTA	22.1	21** 14†		1.44
HEDTA	21.5	1.6	130	1.42
	42.0	3.3	440	2.07
	60.3	5.6	350	2.78
EDTA	10.0	1.17‡		
HEDTA	10.0	0.37‡		

*Viscosity of the 3 mol NaCl/m^3 containing solution is 1.39 relative to the viscosity of water.

**Upper calculated value.

†Lower calculated value.

‡DeBerry et al. (1991).

In Figure 9 the line through the data points of HEDTA is calculated with the experimental reaction rate constants from Table 5. It can be concluded that the fit is satisfactory. For the EDTA complex, however, the characteristics at high pH are surprising: although overall the curve shows the same characteristics as in the case of an instantaneous reaction, the Hatta number decreases above pH = 6 to a somewhat lower level. The solid curve through the data indicates how a theoretical curve should describe the data, whereas the other two curves through the data are calculated from the minimum and maximum value that the reaction rate constant can have (see Table 5 and Figure 9). In the following section, this will be further discussed and the observed reaction rate constants will be compared to those of DeBerry et al. (1991). Figure 10 shows a parity plot of the experimentally observed Hatta numbers for ferric HEDTA and the values calculated from Table 5. Generally, the calculated values of the Hatta number compare well with the experimentally observed values.

Discussion

Reaction between H_2S and OH^-

Above, nothing is said on the reaction of H_2S and OH^-. However, this reaction will occur, often at an instantaneous rate. Then, the maximum enhancement of H_2S absorption due to this reaction follows from:

$$E_A = E_{A\infty} = 1 + He\frac{D_{OH^-}C_{OH^-}}{\nu_B D_A p_A} \tag{10a}$$

From the physical parameters of Tables 3 and 5 it follows that at 22°C and pH = 9 $E_A \approx 1 + 40/p_A$ ($D_{OH} \approx 5.3 \times 10^{-9}$ m^2/s at 25°C, Atkins, 1982). The lowest hydrogen sulfide pressure we applied was about 1,500 Pa. So, the enhancement due to re-

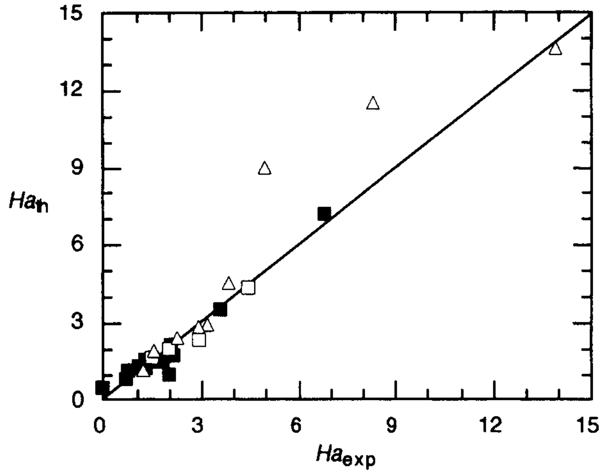

Figure 10. Parity plot of the model values of the Hatta number vs. the experimentally obtained values for the ferric HEDTA complex.

■: $T=21.5°C$, pH=3-10, $C_B=30\text{-}130$ mol/m^3, R.M.S. error=0.18; □: $T=42.0°C$, pH=5-9, $C_B=40\text{-}130$ mol/m^3, R.M.S. error=0.11; △: $T=60.3°C$, pH=4-9, $C_B=40\text{-}130$ mol/m^3, R.M.S. error=0.31.

action with hydroxide is maximally 1.03. Figure 9 shows that at pH = 9 the Hatta number is about 10. Under these conditions E_A will be about equal to the Hatta number. From this, it follows that the observed enhancement of H_2S absorption is entirely due to reaction with ferric chelate. Also at lower pH values, the reaction of hydrogen sulfide with hydroxide under the conditions applied can be neglected.

Only at very low partial pressure of hydrogen sulfide, that is, lower than 40 Pa (400 ppm at atmospheric pressure) at pH = 9, the influence of hydroxide becomes noticeable. As commercial desulfurization plants operate at a pH of about 8 or even lower, this means that the hydrogen sulfide content should be less than 40 ppm at atmospheric pressure before a (minor) part of the enhancement can be ascribed to reaction with hydroxide. This means that only in the case of very deep removal of hydrogen sulfide (to ppm level) combined with a relatively high liquid pH, the hydroxide species plays a significant role in the reaction with hydrogen sulfide.

Reaction mechanism

To explain their experimental results, DeBerry et al. (1991) postulated the following reaction scheme:

$$H_2S + Fe^{3+}(OH^-)L^{n-} \leftrightarrow Fe^{3+}(SH^-)L^{n-} + H_2O \quad (19)$$

$$Fe^{3+}(SH^-)L^{n-} \rightarrow Fe^{2+}L^{n-} + HS^{\bullet} \quad (20)$$

$$HS^{\bullet} + Fe^{3+}(OH^-)L^{n-} \xrightarrow{\text{fast}} Fe^{2+}L^{n-} + S\downarrow + H_2O \quad (21)$$

In reaction 19, hydrogen sulfide reacts with monohydroxy ferric chelate to give the metastable intermediate species $Fe^{3+}LSH$. The existence of this intermediate species was postulated for the ferric chelates of EDTA, HEDTA, DTPA and EGTA by DeBerry et al. (1991) to account for the light absorbance observed at 490 nm when following the reaction between hydrogen sulfide and iron chelate spectrophotometrically. This absorbance at 490 nm could not be ascribed to other species present in solution. According to DeBerry et al. (1991), the intramolecular electron transfer and the subsequent dissociation of this intermediate, that is, Eq. 20, is the rate determining step. The sulfide radical formed in this step then rapidly reacts with ferric chelate to elemental sulfur, Eq. 21. The introduction of the sulfide radical is not further discussed by these authors.

Earlier, Philip and Brooks (1974) studied the formation of iron(III) chelate complexes of hydrogen sulfide and mercaptans in aqueous solution. The equilibrium reaction of hydrogen sulfide with ferric HEDTA complex was found to be best accounted for by the following equation:

$$2Fe^{3+}(OH^-)HEDTA^{3-} + H_2S \leftrightarrow (Fe^{3+}HEDTA^{3-})_2S^{2-} + 2H_2O \quad (22)$$

These authors ascribed the observed absorption peak at 490 nm to the species $(Fe^{3+}HEDTA^{3-})_2S^{2-}$. In contrast to DeBerry et al. (1991), here hydrogen sulfide reacts with two iron chelate ions without the involvement of a sulfide radical. Also, according to the reaction scheme presented by Koch et al. (1986) the reaction of hydrogen sulfide with ferric EDTA does not require the presence of a sulfide radical:

$$HS^- + Fe^{3+}(OH^-)EDTA^{4-} \leftrightarrow Fe^{3+}(OH^-)S^{2-}EDTA^{4-} + H^+ \quad (23)$$

$$Fe^{3+}(OH^-)S^{2-}EDTA^{4-} + Fe^{3+}(OH^-)EDTA^{4-} \leftrightarrow 2Fe^{2+}EDTA^{4-} + S^0 + 2OH^- \quad (24)$$

However, it seems unlikely that a proton is liberated while a hydroxide group is still being attached to the iron complex. Not following the concept of a reaction route through a sulfide radical but taking into account the first-order dependency of the reaction on ferric chelate, we suggest the following reaction scheme:

$$H_2S + Fe^{3+}(OH^-)L^{n-} \overset{k_{-1},k_1}{\leftrightarrow} Fe^{3+}(SH^-)L^{n-} + H_2O \quad (25)$$

$$Fe^{3+}(SH^-)L^{n-} + Fe^{3+}(OH^-)L^{n-} \overset{k_{-2},k_2}{\leftrightarrow} (Fe^{3+}L^{n-})_2S^{2-} + H_2O \quad (26)$$

$$(Fe^{3+}L^{n-})_2S^{2-} \xrightarrow{k_3} 2Fe^{2+}L^{n-} + S\downarrow \quad (27)$$

This reaction scheme contains the equilibrium suggested by Philip and Brooks (1974) while it also explains, if reaction 25 is rate limiting, the first-order dependency of the reaction rate on ferric chelate. Equation 25 is identical to reaction 19 of the scheme of DeBerry et al. (1991). Also the idea of Koch et al. (1986) is expressed by this reaction scheme.

Equilibrium reaction 26 is considered to be very fast with respect to equilibrium reaction 25. For the reaction of hydrogen sulfide with dihydroxy ferric chelate, in the above reaction scheme $Fe^{3+}(OH^-)L^{n-}$ should be replaced by $Fe^{3+}(OH^-)_2L^{n-}$ and H_2O by $H_2O + OH^-$. The surplus hydroxide liberated may react with monohydroxy ferric chelate to dihydroxy ferric chelate, depending on K_B (see Eq. 13).

Instantaneous reaction regime

In light of the observed first-order rate dependency on hydrogen sulfide and on ferric chelate, the rate determining step is reaction Eq. 25. As ν_B in the terms $D_B/\nu_B D_A$ and $\sqrt{D_B}/\nu_B\sqrt{D_A}$ is the stoichiometric coefficient of the rate determining step, it follows that $\nu_B = 1$. Now the ratio of the diffusivity of ferric chelate relative to the diffusivity of hydrogen sulfide can be calculated. From Table 4 it follows that:

$$\text{EDTA:} \quad D_B/D_A = 0.30 \tag{28a}$$

$$\text{HEDTA:} \quad D_B/D_A = 0.49 \tag{29a}$$

for film model and:

$$\text{EDTA:} \quad D_B/D_A = 0.09 \tag{28b}$$

$$\text{HEDTA:} \quad D_B/D_A = 0.24 \tag{29b}$$

for the penetration theory. This result is unexpected, because we previously found (Wubs and Beenackers, 1993) that the ratio of the diffusivity of ferrous chelate relative to the diffusivity of oxygen was equal to 0.183 for both the ferrous chelate of EDTA and the ferrous chelate of HEDTA, independent of temperature. Moreover, it was shown that ion charge of the complex had no influence. Therefore, also here the ratio D_B/D_A is expected to be the same for both EDTA and HEDTA ferric chelates. According to the Stokes-Einstein equation, this ratio of diffusivities does not depend on viscosities. Therefore, the diffusivities of the ferric chelates in water can be calculated from the diffusivity of hydrogen sulfide in water ($D_A = 1.79 \cdot 10^{-9}$ m^2/s at 22°C, Haimour and Sandall, 1984). For the ferric chelates of EDTA and HEDTA it then follows that at 22°C:

$$\text{EDTA:} \quad D_B = 0.54 \cdot 10^{-9}\ \text{m}^2/\text{s} \tag{30a}$$

$$\text{HEDTA:} \quad D_B = 0.88 \cdot 10^{-9}\ \text{m}^2/\text{s} \tag{31a}$$

again for film model:

$$\text{EDTA:} \quad D_B = 0.16 \cdot 10^{-9}\ \text{m}^2/\text{s} \tag{30b}$$

$$\text{HEDTA:} \quad D_B = 0.42 \cdot 10^{-9}\ \text{m}^2/\text{s} \tag{31b}$$

and for penetration theory. For the ferrous chelates of EDTA and HEDTA the observed D_B/D_{O_2} of 0.183 (Wubs and Beenackers, 1993) in combination with the diffusivity of oxygen in water of $2.14 \cdot 10^{-9}$ m^2/s at 22°C (St-Denis and Fell, 1971) results for both species in:

$$\text{EDTA, HEDTA:} \quad D_B = 0.39 \cdot 10^{-9}\ \text{m}^2/\text{s} \tag{32}$$

Earlier, also O'Connor et al. (1971) found the diffusivity of the monohydroxy form of ferric EDTA to be $0.39 \cdot 10^{-9}$ m^2/s. It follows that the diffusivities found above with either model differ too much from literature data. Since the diffusivities of both ferric complexes can be expected to be about equal, it also follows that the two diffusivities predicted from each model are not consistent. Since the difference in D_B for EDTA and HEDTA are the smallest from the predictions based on the film model, it appears that the film model probably is the preferred model here. Moreover, for the system of this study one may question if the penetration theory may be applied at all. The idea of the penetration model of Higbie is that a fluid element arrives at the gas-liquid interface, stays there for a while, absorbing gas, and finally returns to the bulk of the liquid to mix up. It is replaced by a fresh fluid element, with concentrations according to bulk-liquid conditions. This idea means that all sulfur produced in an element will also be transferred to the bulk of the liquid. However, when carrying out the experiments, we observed that when the stirring rate was too low, sulfur preferentially remained at the gas-liquid interface, though the stirring rate was high enough to ensure the bulk to be well mixed and the mass-transfer coefficient to be in the order of $2\text{-}3 \cdot 10^{-5}$ m/s. Once sulfur is returned to the bulk, chances are small that it returns to the gas-liquid interface because of agglomeration to larger particles. Towards the end of such an experiment the whole gas-liquid interface could be covered by sulfur. This phenomenon cannot be described by penetration theory, as the time to accumulate sulfur at the gas-liquid interface by far exceeded the specific contact time of a liquid penetration element. Therefore, we conclude that the diffusivities of hydroxy ferric chelates found in this work are probably too high. If so, this means that diffusivity alone cannot be responsible for the observed absorption enhancement, but also that at least one more factor plays a role in extra enhancing the absorption of hydrogen sulfide. A possible factor could be charge effects during transport of the reactive ions. However, the ferrous chelate products have the same charge as the ferric chelate substrates (except for the dihydroxy species) and the diffusivities of the ferric and ferrous chelates are about the same. Therefore, charge effects can be excluded.

Another possible factor that may result in too high apparent diffusivities is the presence of sulfur near the gas-liquid film. Mehra and Sharma (1988) showed that the reactive absorption of hydrogen sulfide into a iodine containing solution showed enhancements factors substantially higher above those following from instantaneous reaction of hydrogen sulfide with iodine alone. They concluded that the additional enhancement was caused by adsorption of hydrogen sulfide on sulfur formed *in situ*. Though these effects are not yet explained quantitatively (see Wubs et al., 1990) we conclude that also in the reactive absorption of H_2S in ferric chelate solutions extra enhancement due to coadsorption of H_2S on sulfur formed *in situ* might have occurred. A recent article of Clarke et al. (1992) indicates that the formation of polysulfides provides an alternative mechanism for the mechanism proposed by Mehra and Sharma (1988). Comparing the Eqs. 30-32 and assuming equal diffusivities for ferric and ferrous chelates, the maximal possible extra enhancement due to H_2S adsorption on sulfur probably is 1.38 for EDTA and 2.26 for HEDTA. However, additional research is required to check whether enhancement has actually occurred.

Apart from the "diffusivity coefficients," equilibrium constants are also obtained from the instantaneous reaction regime. From Table 4 it appears that the values found for the HEDTA complex at 21.5°C agree with the results of Gustafson and Martell (1963). Also, the change of the constants with temperature seems to be consistent; however, due to lack of literature data at higher temperatures, a definite conclusion cannot be made yet. A large difference, however, exists be-

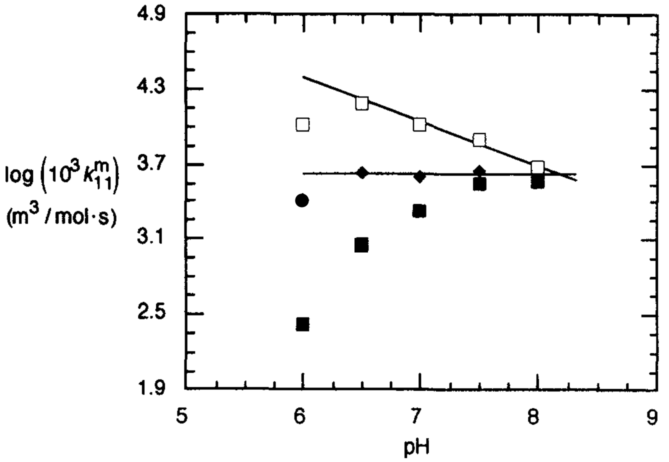

Figure 11. k_{11}^m **of the ferric EDTA complex as function pH.**

■: original data of DeBerry et al. (1991); □: corrected data of DeBerry et al. (1991) using K_A from Gustafson and Martell (1963); ◆: corrected data of DeBerry et al. (1991) using $\log K_A = 7.2$ (this work).

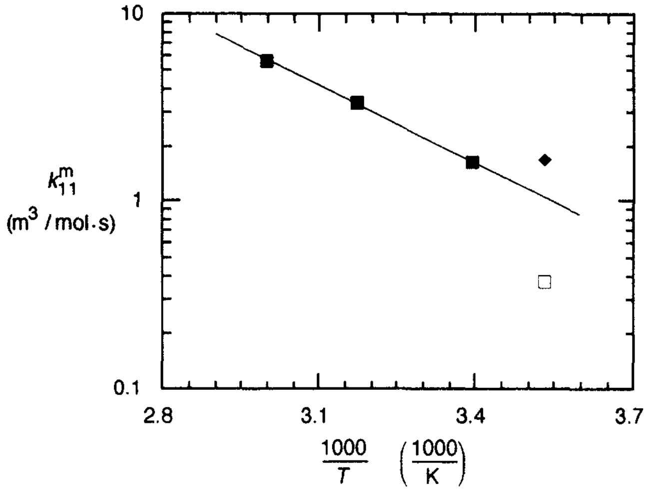

Figure 12. Arrhenius plot for k_{11}^m **of the ferric chelate of HEDTA.**

■: this work; □: DeBerry et al. (1991) (uncorrected); ◆: DeBerry et al. (1991) (corrected, see text).

tween our measured value of the equilibrium constant K_A of the EDTA complex and the value given by Gustafson and Martell (1963). Since latter authors carried out their experiments in a 1 kmol/m³ KCl solution, this difference may be due to differences in activity coefficients. As no ion-specific parameters are available for calculating the activity coefficients of iron complexes, more advanced models, such as the Pitzer model, cannot be applied. The more simple Davies equation (Nancollas and Tomson, 1982) does not require such specific parameters but is only accurate at low ion strengths. The calculated activity coefficients with this equation are accurate within 1% for ion strengths up to 0.2 kmol/m³. Estimating these activity coefficients with the Davies model showed that the value of Gustafson and Martell (1963) increased by about 0.1 for EDTA. This is far less than the difference of 1.4 with our value.

The difference between these two values of K_A for EDTA becomes striking if the results of DeBerry et al. (1991) are analyzed. In Figure 11, their original experimental values of k_{11}^m of the EDTA complex are shown as function of the pH together with the corrected values the authors obtained by accounting for the reactive species being the monohydroxy form. For this correction they used the value for K_A, as given by Gustafson and Martell (1963). It can be seen that the corrected data still exhibit a pH dependency whereas according to reaction Eq 19 such a dependency is not expected. From assuming that k_{11}^m must be independent of pH, a new correction can be made. The new value thus obtained for k_{11}^m is 4.07 m³/mol·s, which is much closer to our experimental results, and the new value for $\log K_A$ becomes 7.6, which is very close to the value we found experimentally (see Table 4). We therefore conclude that our value of this equilibrium constant most likely is the more accurate result.

Reaction kinetical results

Figure 12 shows the observed temperature dependency of the rate constant for the reaction of hydrogen sulfide with monohydroxy ferric chelate of HEDTA according to the equation:

$$k_{11}^m = k_{11,0}^m e^{-Ea/RT} \qquad (33)$$

with: $Ea = (26.4 \pm 0.6)$ kJ/mol and $k_{11,0}^m = 7.8 \cdot 10^4$ m³/mol·s. For comparison the value reported by DeBerry et al. (1991) is shown too. Probably the latter value has not been corrected for the presence of different types of hydroxy components. Although these authors recognize the presence of significant amounts of monohydroxy dimer and the possible formation of the dihydroxy form, no correction for these species seems to have been made. At pH = 6.5 and 10°C, DeBerry et al. (1991) reported k_{11}^m to be 0.37 m³/mol·s. Extrapolation to 10°C of the values of K_A and K_D given in Table 4 gives $\log K_A = 10$ and $\log K_D = 2.5$ m³/kmol. From Eqs. 15-17 it can now be calculated that the ratio of the concentration of monohydroxy ferric chelate to the total concentration of ferric chelate, that is, C_B^m/C_B, equals 0.22 at the maximum concentration used by DeBerry et al. (1991). Correction for this ratio gives $k_{11}^m = 1.7$ m³/mol·s, which is also presented in Figure 12. The value of $C_B^m/C_B = 0.22$ increases to $C_B^m/C_B = 1$ if the dimer is absent or if the actual concentration of ferric chelate approaches zero ($C_B \rightarrow 0$ in Eq. 17). It, therefore, can be concluded that our kinetic results are not in conflict with the rate constant of DeBerry et al. (1991), provided their result is corrected for the active amount of ferric chelate.

Returning to Figure 9, it appears that above a certain pH the experimental Hatta numbers for the ferric EDTA complex no longer can be described by Hatta numbers calculated from the rate constants given in Table 5. Above pH ≈ 7, the experimental Hatta number decreases again with increasing pH and it seems that an additional reaction, influenced by the pH, starts to interfere. Several hypothesis for this phenomenon can be raised.

It could be that at higher pH-values, one of the reactants or reactive intermediate starts to form another hydroxy component. As shown above, the conversion of H_2S to HS^- by reaction with hydroxide is negligible. Also, the formation of a dihydroxy component of ferric EDTA can be disregarded because this species has not been found. Perhaps, one of the sulfur containing reactive intermediates can form a less reactive hydroxy-component. This is a possibility which cannot be excluded. In the high-pressure regime, the reaction is fully diffusion limited, so that such a change in reactivity might not be observed there.

Another possibility would be that Fe^{2+}EDTA equilibrates with Fe^{2+}(OH)EDTA which in turn may interfere with the reaction in some way. This ferrous hydroxy EDTA equilibrium was reported by Schwarzenbach and Heller (1951); however, Bull et al. (1983) and Clark and Martell (1987) could not reproduce the Fe^{2+}(OH)EDTA species. Clark and Martell (1987) therefore argued that the result of Schwarzenbach and Heller was subject to experimental errors. The influence of possible interference of sulfur is not known, but probably is much less than in the high pressure regime due to much lower absorption rates and thus lower sulfur production rates.

Conclusions

The reaction of hydrogen sulfide with ferric chelates of EDTA and HEDTA is first-order in both hydrogen sulfide and ferric chelate. Only the hydroxy forms of the ferric chelates are reactive with hydrogen sulfide, and the dihydroxy form of the HEDTA complex is much more reactive than the monohydroxy form. The dimer of monohydroxy ferric HEDTA probably is not reactive. The reaction rate constants follow the sequence:

$$Fe^{3+}(OH)_2HEDTA \gg Fe^{3+}(OH)EDTA \gg Fe^{3+}(OH)HEDTA$$

Both the experimentally observed hydroxy equilibrium constants and the rate constants for the monohydroxy ferric EDTA and HEDTA complexes with hydrogen sulfide are consistent with the scarce data reported in literature.

Acknowledgment

We acknowledge financial support of Shell Internationale Petroleum Maatschappij B. V., The Hague, Netherlands, and of the Foundation for Chemical Research in the Netherlands (SON), a division of the Dutch Organization for Scientific Research.

Notation

a = gas-liquid contact area, m^2
C = concentration in the bulk of the liquid, mol/m^3
C^i = concentration at gas/liquid interface = solubility, mol/m^3
D = diffusivity, m^2/s
Ea = activation energy, kJ/mol
E_A = enhancement factor of H_2S absorption
$E_{A\infty}$ = enhancement factor of H_2S absorption at instantaneous reaction rate
He = Henry coefficient, $Pa \cdot m^3/mol$
Ha = Hatta number
J_A = mass-transfer rate of hydrogen sulfide, $mol/m^2 \cdot s$
k_{11} = reaction rate constant, $m^3/mol \cdot s$
K_A = first hydroxylation equilibrium constant, $m^3/kmol$
K_B = second hydroxylation equilibrium constant, $m^3/kmol$
K_D = dimer formation equilibrium constant, $m^3/kmol$
k_L = mass-transfer coefficient without reaction, m/s
$k^m_{11,0}$ = preexponential factor, $m^3/mol \cdot s$
n = charge number of chelant
p = pressure, Pa
R = gas constant = 8.31441, $J/mol \cdot K$
t = time, s
T = temperature, K
V = volume, m^3

Greek letters

ν_B = stoichiometry of the rate limiting reaction step

Subscripts

A = hydrogen sulfide
B = ferric chelate
G = gas phase
L = liquid phase
OH = hydroxide anion
∞ = at t = infinity

Superscripts

a = active
d = dihydroxy ferric chelate
m = monohydroxy ferric chelate
O = at $t = O$

Literature Cited

Asai, S., Y. Konishi, and T. Yabu, "Kinetics of Absorption of Hydrogen Sulfide into Aqueous Ferric Sulfate Solutions," *AIChE J.*, **36**, 1331 (1990).

Atkins, P. W., *Physical Chemistry*, 2nd ed., Oxford Univ. Press, Oxford (1982).

DeBerry, D. W., B. Petrinec, and T. Trofe, "New Insights from Investigation of Fundamental Mechanisms of Liquid Redox Chemistry," Liq. Red. Sulf. Rec. Conf., TX (1991).

Buenger, C. W., S. A. Bedell, and L. H. Kirby, "Chelates in H_2S Removal," Laur. Reid Gas Cond. Conf., OK (Mar. 1988).

Bull, C., G. J. McClune, and J. A. Fee, "The Mechanism of Fe-EDTA Catalyzed Superoxide Dismutation," *J. Am. Chem. Soc.*, **105**, 5290 (1983).

Chang, C.-S., and G. T. Rochelle, "Mass Transfer Enhanced by Equilibrium Reactions," *Ind. Eng. Chem. Fundam.*, **21**, 379 (1982).

Clark, N. H., and A. E. Martell, "Ferrous Chelates of EDTA, HEDTA and SHBED," *Inorg. Chem.*, **27**, 1297 (1988).

Clarke, E., A. E. Martell, D. McManus, and T. Solouki, "Investigation of the Role of Polysulfides in Sulfur Formation Mechanisms in Iron-Based Liquid Redox Processes," GRI Liquid Redox Sulfur Rec. Conference, Austin, TX (Oct. 5-6, 1992).

DeCoursey, W. J., "Absorption with Chemical Reaction: Development of a New Relation for the Danckwerts Model," *Chem. Eng. Sci.*, **29**, 1867 (1974).

Gustafson, R. L., and A. E. Martell, "Hydrolytic Tendencies of Ferric Chelates," *J. Phys. Chem.*, **67**, 576 (1963).

Haimour, N., and O. C. Sandall, "Molecular Diffusivity of Hydrogen Sulfide in Water," *J. Chem. Eng. Data*, **29**, 20 (1984).

Koch, S., G. Ackermann, and K. Schüller, "Über ternäre Komplexe von Eisen(III) mit Aminopoly-carbonsäuren und Sulfid," *Z. Chem.*, **26**, 339 (1986).

Mehra, A., and M. M. Sharma, "Absorption of Hydrogen Sulfide in Aqueous Solutions of Iodides Containing Dissolved Iodine: Enhancements in Rates Due to Precipitated Sulphur," *Chem. Eng. Sci.*, **43**, 1071 (1988).

Nancollas, G. H., and M. B. Tomson, "Guidelines for the Determination of Stability Constants," *Pure Appl. Chem.*, **54**, 2675 (1982).

Novikov, G. I., I. A. Belov, and P. K. Rud'ko, "Kinetics of Hydrogen Sulfide Oxidation by an Aqueous Solution of Iron(III) Chloride," *Vesti Akad. Navuk BSSR, Ser. Khim. Navuk*, **6**, 44 (1984).

O'Conner, G. A., W. L. Lindsay, and S. R. Olsen, "Diffusion of Iron and Iron Chelates in Soil," *Soil Sci. Soc. Amer. Proc.*, **35**, 407 (1971).

Philip, C. V., and D. W. Brooks, "Iron(III) Chelate Complexes of

Hydrogen Sulfide and Mercaptanes in Aqueous Solution," *Inorg. Chem.*, **13**, 384 (1974).

Schwarzenbach, G., and J. Heller, "Komplexone XVIII. Die Eisen(II)- und Eisen(III)-komplexe der Äthylendiamin-tetraessigsäure und ihr Redoxgleichgewicht," *Helv. Chim. Acta*, **34**, 576 (1951).

St-Denis, C. E., and C. J. D. Fell, "Diffusivity of Oxygen in Water," *Can. J. Chem. Eng.*, **49**, 885 (1971).

Versteeg, G. F., and W. P. M. van Swaaij, "Solubility and Diffusivity of Acid Gases (CO_2, N_2O) in Aqueous Alkanolamine Solutions," *J. Chem. Eng. Data*, **33**, 29 (1988).

Westerterp, K. R., W. P. M. van Swaaij, and A. A. C. M. Beenackers, *Chemical Reactor Design and Operation*, Wiley, New York (1984).

Wilke, C. R., and P. Chang, "Correlation of Diffusion Coefficients in Dilute Solutions," *Am. Inst. Chem. Eng. J.*, **1**, 264 (1955).

Wubs, H. J., A. A. C. M. Beenackers, and R. Krishna, "Absorption of Hydrogen Sulfide in Aqueous Solutions of Iodine—A Critical Review," *Chem. Eng. Sci.*, **46**, 703 (1990).

Wubs, H. J., and A. A. C. M. Beenackers, "The Kinetics of the Oxidation of Ferrous Chelates of EDTA and HEDTA in Aqueous Solution," *Ind. Eng. Chem. Res.*, **32**, 2580 (1993).

Manuscript received Jan. 25, 1993, and revision received July 5, 1993.